

380 kV Corona Ring Optimization for ac Voltages

Suat Ilhan and Aydogan Ozdemir

Istanbul Technical University
Department of Electrical Engineering
34469, Maslak, Istanbul, Turkey

ABSTRACT

This paper presents corona ring optimization for 380 kV V-insulator string composed of glass insulator units. The influence of the corona ring design parameters are examined not only with regard to 3D simulations but also laboratory tests. The purpose of the simulations is to find reasonable corona ring design parameters such as corona ring diameter, corona tube diameter and installation height on the point of effective field regulation around the critical region of the string. Indoor laboratory tests including radio interference voltage levels, corona inception voltages and ac flashover voltages are conducted on the centre phase of a full scaled tower both for experimental based corona ring design as well as verifications of the simulations. After both simulations and experimental based investigations, appropriate corona ring design parameters for the string are determined for effective field regulation, minimum interference level, ac flashover performance and economic point of view.

Index Terms — ac flashover, corona ring, electric field, radio interference.

1 INTRODUCTION

CORONA discharges become an important design factor not only because of corona losses they cause and also due to the electromagnetic interferences commonly known as radio interferences [1]. Electric field strengths in the vicinity of the insulators are crucial to prevent excessive radio interference levels and probable corona discharges. Insulator strings are equipped with corona rings to minimize the corona discharges and radio interferences which are mainly caused by insulators and insulator-metal conjunctions. Corona rings are also designed to regulate the field distributions along the strings [2, 3] and to protect the insulator string from direct power arcs [4]. However, all these issues are strongly dependent on the corona ring design parameters.

Recent papers regarding corona ring optimization have presented only 2D [2] and 3D [3] computer simulations especially for vertically mounted insulator strings. However, effects of grading rings and their design parameters on ac and RIV performance of V-insulator string have not been sufficiently evaluated experimentally so far. Moreover, there is not a compact optimization effort so far combining simulations and laboratory tests based corona ring optimization for ac excitations.

The purpose of this study is therefore to optimize the geometrical dimensions and installation location of corona rings of V-insulator strings both for 3D electrostatic simulation studies and indoor laboratory tests under ac voltages. The V-insulator string under investigation is used in

380 kV Turkish National Power Transmission System comprising 20 unit cap-and-pin type glass insulator units. The studies were carried out two different types of grading devices: Racket type, R-type and circular type, C-type grading devices.

3D simulations were conducted to determine the optimum design parameters that minimize the maximum field gradients and as well as effective field regulation at the critical regions of the string. Effects of conductor lengths, conductor sags, existence of adjacent phases and ground wires were also taken into consideration for more applicable solutions.

Indoor laboratory tests were performed at Fuat Kulunk High Voltage Laboratory of Istanbul Technical University. Laboratory model was constructed for the central phase of the system as being the worst one from the point of voltage distribution and maximum field strength. Radio interference voltage (RIV) levels, visible corona inception voltages and ac flashover voltages were determined for different ring design parameters. Flashover routes were also recorded to attain fair conclusions. The test based optimum solutions were then compared with the previous simulation based solutions to confirm the concordance between the results.

2 MODEL PARAMETERS

Figure 1 shows the basic dimensions of the transmission tower used in 380 kV transmission systems. It carries 3x1272 MCM pheasant conductors of 35 mm in diameter (triple bundle with bundle diameter of 500 mm) and ground wires of Ø10 mm. Each branch of V-insulator string consists of 20 cap-and-pin type toughened glass insulators as shown in Figure 1.

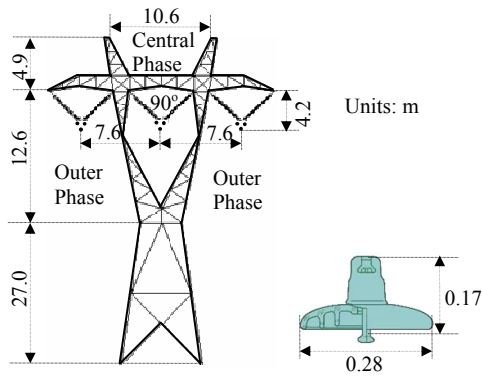
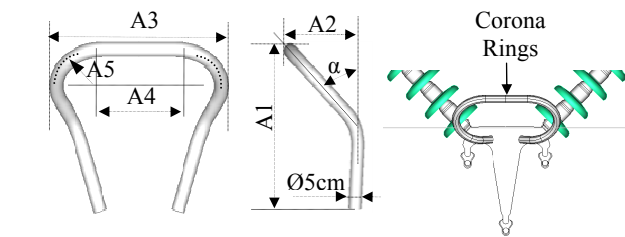


Figure 1. Basic dimensions of 380 kV suspension type transmission tower and cap-and-pin type glass insulator unit.

Figure 2 and Figure 3 show different R-type rings and circular C-type corona rings with basic design parameters, respectively.



Model Name	Model Parameters (cm)					
	A1	A2	A3	A4	A5	α°
R1	53,5	32,0	60,0	24,0	18,0	27
R2	48,0	25,0	50,0	13,0	18,5	30
R3	46,0	24,0	50,0	0,0	25,0	25
R4	42,0	26,0	70,0	26,0	22,0	70
R5	41,0	32,0	70,0	27,0	21,5	30

Figure 2. R-type corona rings and design parameters.

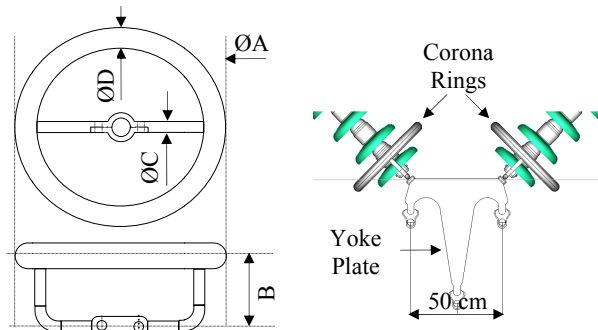


Figure 3. C-type corona ring and design parameters.

R-type rings are the common corona rings for V-insulator strings composed of cap-and-pin type insulators. In this study, five different R-type rings with different design parameters were simulated and tested. Although only R5 type ring is used currently together with the string under the study, the other R-type rings were also investigated to see the detailed effects of R-type ring parameters on ac performance of the string.

Depending upon the past experience of the utility staff and also geometric feasibility of the design, optimization parameters are selected as follows for C-type corona rings.

- A: Corona ring diameter = 40, 45, 50, 55, 60 and 65 cm;
- B: Installation height = 0, 5, 10, 15, 20 and 25 cm;
- C: Inner tube diameter = 2.5 cm constant;
- D: Ring tube diameter = 4, 4.5 and 5 cm.

C-type grading devices are also common rings, especially for composite insulator strings. Therefore, the results of the study are not limited to only 380 kV V-insulator string and may be useful and applicable for transmission lines operating under different voltages.

3 SIMULATION STUDIES

Simulation studies cover electric field strength calculations in the vicinity of the insulator string. Simulations were performed both for a practical model and for a simplified laboratory model. Optimum corona ring settings were determined with respect to the lowest maximum field gradients at the critical regions of the string. Maximum electric field stresses in the area of live end side were evaluated more precisely as being the critical region of the system.

A conducting earth plane (100 m x 100 m) was placed under the transmission tower. The instantaneous voltages ($380 \times \sqrt{2}/\sqrt{3} = 310.27 \text{ kV}_{\text{peak}}$, (peak value of line-to-ground voltage) of 50 Hz were applied to the three-phase transmission system. All the calculated electric field strengths were expressed in peak or maximum value, $\text{kV}_{\text{peak}}/\text{cm}$, kV_p/cm .

In addition to corona ring design parameters, several secondary parameters affect the field distributions around the string to some extent. Conductor length effects have been introduced by Zhao and Comber [5]. Here, all the secondary factors including conductor sags, existence of adjacent phases and ground wires were also taken into consideration for an improved representation of the actual service conditions. Potential distributions along the insulator strings for different conductor lengths are shown in Figure 4.

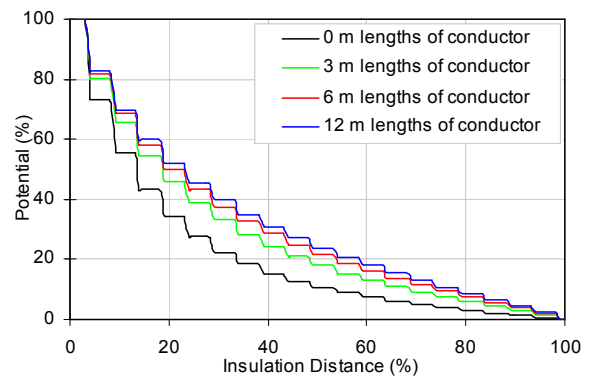


Figure 4. % potential distribution along the 380 kV V-string.

Equipotential lines for a conductor length of 25 m are illustrated in Figure 5. Simulations showed that the effect of conductor lengths on the voltage distribution and on the field

strengths decreases as the conductor length increases. The differences become negligible (<0.5 %) for the conductor lengths of 25 m and above. For example, maximum electric field strengths, E_{max} , on the surface of R1 type corona ring are found to be 32.06, 22.55, 20.14, 19.21, 18.98 and 18.98 kV_p/cm for 0, 3, 6, 12, 25 and 50 m lengths of phase conductors, respectively.

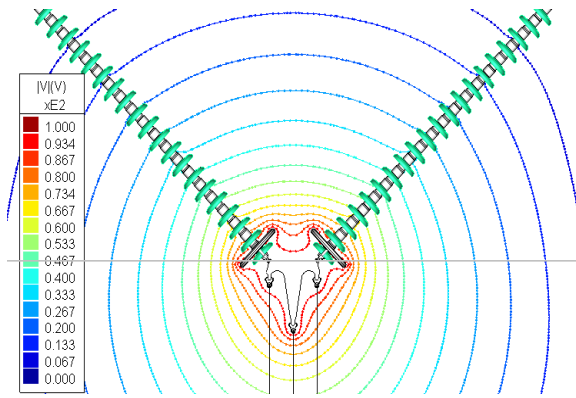


Figure 5. % equipotential lines for the 380 kV V-string.

Conductor sags of longer lines affect the field distribution. Conductor sags in this study were approximated by parabola equation [6]. The distance between the two adjacent towers of equal heights is assumed to be 450 m. E_{max} on R1 type grading ring was calculated to be 18.98, 19.39, 19.76 and 20.17 kV_p/cm for 0, 5, 10, 15 and 20 m of maximum conductor sags, respectively. These pre-simulations showed that increasing conductor sags give higher field strengths on the corona rings as well as on the other critical regions.

Pre-simulations were also performed to include the effects of adjacent lines. E_{max} on R1 type corona ring was found to be 19.26 and 20.17 kV_p/cm for a single centre phase and for three-phase excitations, respectively. These results show that the existence of adjacent phases increases the maximum field strength nearly by 5 %. Moreover, potential distribution along the string is found to be more uniform for a single isolated phase. Finally, pre-simulations showed that the existences of ground wires have negligible effect (< 0.01 %) on the field distributions.

According to pre-simulation results, 25 m of conductor length, three-phase excitation and 15 m of maximum conductor sags which are the probable one are found to be the reasonable values representing the actual service conditions and are used as the reference parameters for the remaining ac simulations.

Simulations were performed both for the service model and for the simplified laboratory model which are shown in Figure 6. All the secondary factors were taken into account in service model simulations. However, simulations were performed for the central phase while neglecting the adjacent phases, conductor sags and earth wires for the laboratory model because of the laboratory size limitation. Insulator units were modeled by glass dielectric mediums and metal parts while neglecting the cement fillings. Moreover, round insulator

sheds were sharpened for the sake of less modeling elements. These two simplifications were found to be less effective on the field distributions by some additional tests.

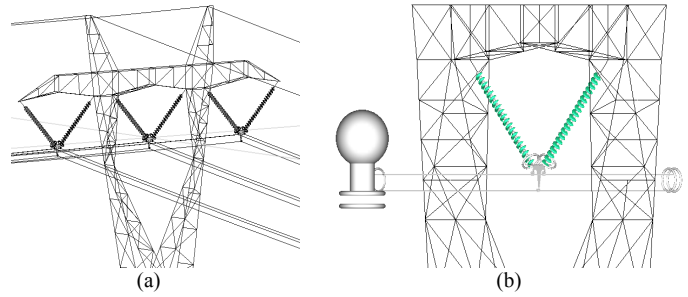


Figure 6. (a) Service model including all affective factors (b) Laboratory model including only the centre phase of the string.

Simulations showed that there were some critical regions in the vicinity of highly stressed live end side of the string where the field strengths were much greater than the ones on the other sides of the system. Optimization procedure was therefore concentrated on these critical regions and aims to minimize the associated maximum field strengths. Critical regions designated by K, L, M and N are shown in Figures 7 - 8. Since corona inception changes the field distribution around the string, 3D simulations are used as a starting point of the investigations [7]. In the simulations, insulator surfaces are assumed to be dry and clean.

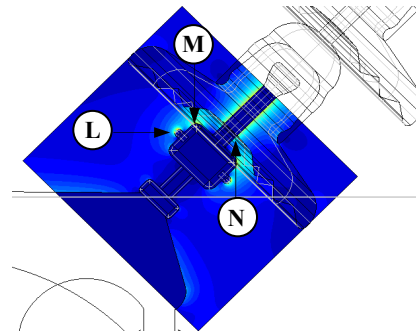


Figure 7. Critical regions of the string.

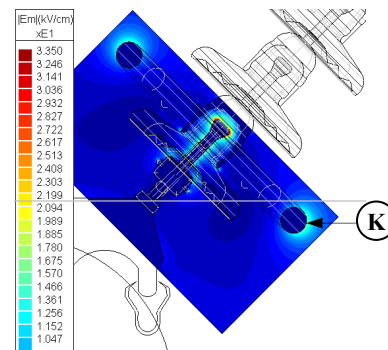


Figure 8. E_{max} density around the critical regions for C-type ring (A = 50 cm, B = 15 cm, D = 5 cm).

Simulations were first performed for without corona ring case. 39.31, 30.94 and 15.33 kV_p/cm field results were obtained for Regions-L -M and N, respectively. Detailed field results under different ring design parameters are given in Figure 9 - 18 for service case model.

Figure 9 and Figure 10 illustrate E_{max} on corona ring surface (Region - K) versus installation height. It is obvious that the increasing corona tube diameter improves the field strengths on the corona rings. Nearly 11 percent field reductions were obtained between the field results for 4 and 5 cm tube diameters. Figure 10 shows that the increase in parameter B results in a linear increase in E_{max} .

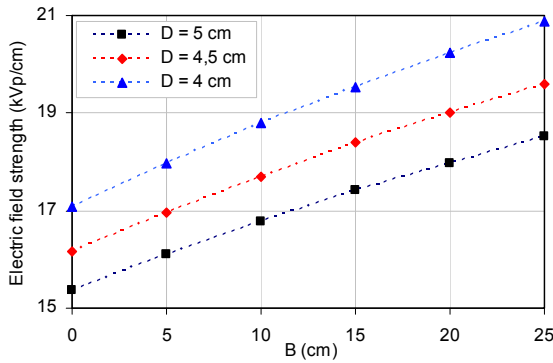


Figure 9. E_{max} on corona ring surface (A = 50 cm).

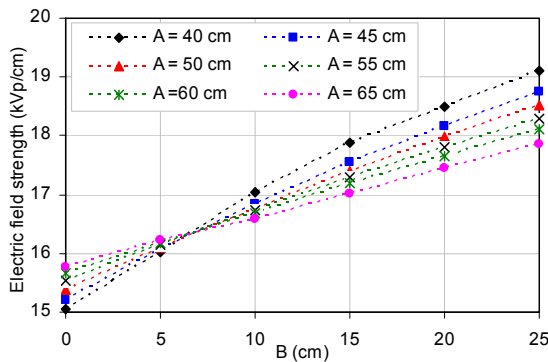


Figure 10. E_{max} on corona ring surface (D = 5 cm).

Figure 11 and Figure 12 show the E_{max} on Region-L versus ring parameters. It is clear that E_{max} decreases for increasing ring tube diameters. Up to 8 % reductions were observed transition of tube diameter from 4 cm to 5 cm. However, E_{max} versus installation height shows a minimum around B = 10 - 15 cm which can be considered to be an optimal value for the regional stress.

Maximum field strengths on Region-M are illustrated in Figure 13 and Figure 14. Increasing ring tube diameter decreases the fields on this region. Maximum 7 % reductions were seen between the tube diameter of 4 and 5 cm. E_{max} decreases with an increasing installation height as shown in Figure 14. However, decreasing rate decreases after an installation height of 10 - 20 cm. 20 cm and greater

installation heights do not bring significant improvement in the field strengths of this zone.

Finally, E_{max} on Region-N are illustrated in Figure 15 and Figure 16. Effect of parameter D is shown in Figure 15 and field differences between 4 and 5 cm of D are about 5 percent. As shown in Figure 16, the field strength decrease for an increasing installation height is more regular here. Actually, E_{max} in this zone are considerably small when compared with those of the other zones. However, laboratory tests showed that the visible corona discharges at the region starts shortly after the visible corona inception at Regions-L and M. The discordance of simulation results and the laboratory tests are mainly because of simplified modeling of the cement-glass conjunction zone.

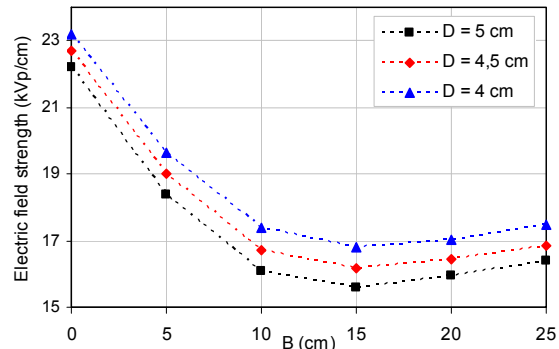


Figure 11. E_{max} on Region-L (A = 50 cm).

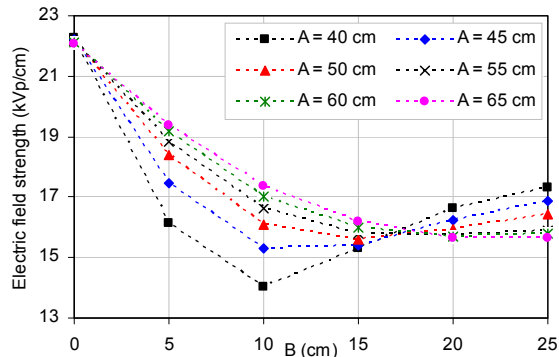


Figure 12. E_{max} on Region-L (D = 5 cm).

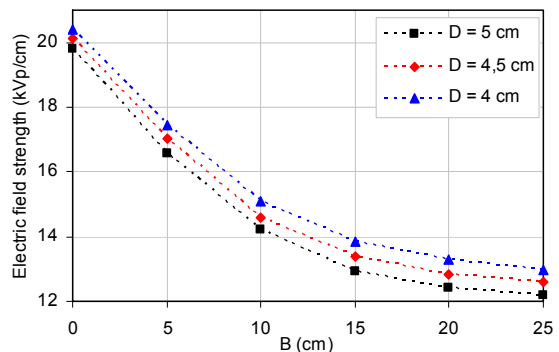


Figure 13. E_{max} on Region-M (A = 50 cm).

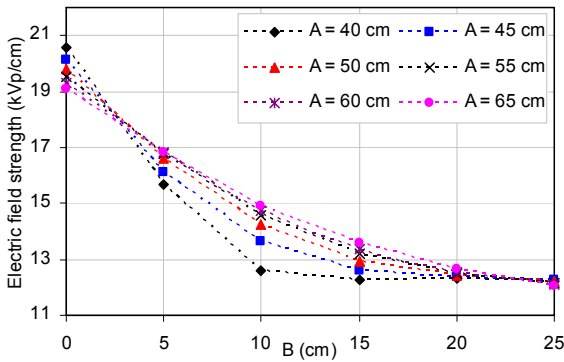


Figure 14. E_{max} on Region-M ($D = 5$ cm).

It is clear from the previous illustrations that increasing corona ring tube diameter decreases E_{max} at all critical zones. Among them, corona ring surface field strength, Region-K, is more sensitive to ring tube diameter when compared with the others.

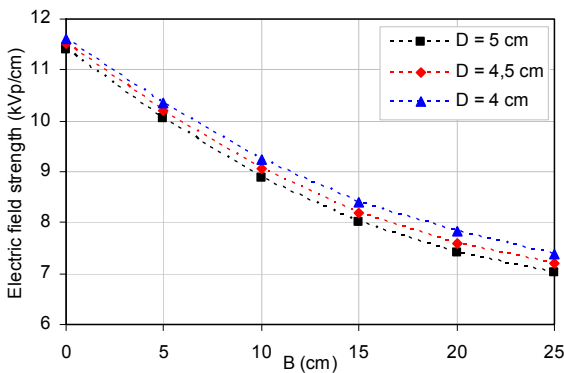


Figure 15. E_{max} on Region-N ($A = 50$ cm).

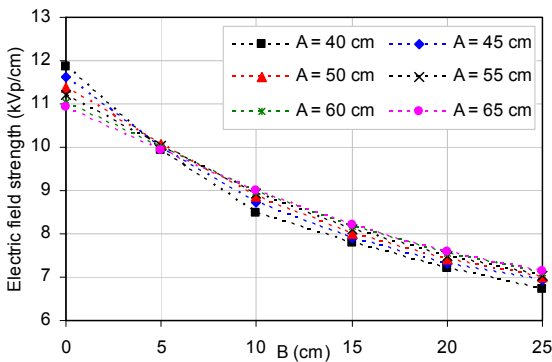


Figure 16. E_{max} on Region-N ($D = 5$ cm).

Under normal conditions, maximum electric field is expected to occur on corona ring surfaces. Otherwise, it cannot effectively be controlled by the grading devices. However, for some corona ring design parameters, E_{max} seems to occur at other critical regions rather than corona ring itself. $B = 0$

mounting height is the example to this situation. Figure 17 shows E_{max} values on the critical regions for the ring of 50 cm diameter. It is clear from the figure that the installation heights should be equal or greater than 10 cm for an effective field control. 5 cm or larger B is required for the ring diameters of 40 cm and the value of the B should be 15 cm for corona rings with 65 cm diameter for the effective usage of the ring. In summary, value of B is dependent on the corona ring diameter and the larger the corona ring diameters, the larger the installation heights for the proper dimensioning of the ring.

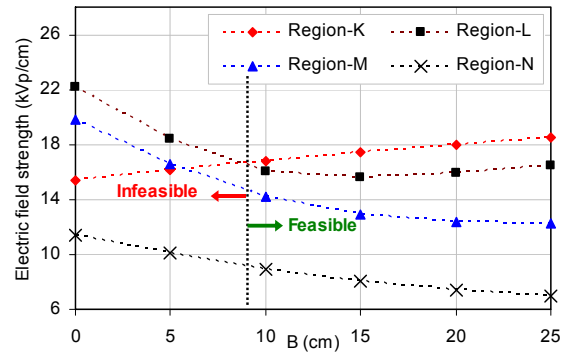


Figure 17. E_{max} versus installation height for a C-type ring ($A=50$ cm, $D=5$ cm).

On the other hand, corona tube diameter is also an important design parameter especially for the maximum field variation on the ring surface. As the corona tube diameter decreases, smaller mounting heights are sufficient for an effective field control and opposite are also true. However, corona rings with small tube diameter may produce its own corona discharge. Therefore, E_{max} on the ring surface should not exceed corona inception electric field under both operating and RIV measurement voltages. $D < 4$ cm is not reasonable because of the maximum field occurrence on the ring surface and $D > 5$ cm may not also be appropriate because of both larger B parameters for effective field control and economic point of view.

E_{max} at critical regions of the strings equipped with R-type rings are shown in Figure 18. Maximum field strengths on Region-K occur on A5 arc segment (see Figure 2) for all R-type rings. E_{max} at critical regions are greater than those obtained for C-type rings. R-type corona rings with larger A3 parameters show better field regulation for Regions-L, M and N as shown in Figure 18 since increasing A3 parameter results in a good coverage of the critical regions by the rings. R5 type ring is the best one providing the minimum field gradients. However, maximum field strengths on Region-L and M are greater than the corresponding values on corona ring surfaces. Therefore, none of the R-type rings provide an effective maximum field strength regulation. Although R5 type ring, which is currently used together with the string, satisfies the required both RIV ($\leq 500 \mu V$ at 277 kV_{rms} test voltage) and ac performances (1 minute ac withstand voltage ≥ 620 kV_{rms}) as explained in the tests, its field regulation effect need to be improved further to use the ring more efficiently.

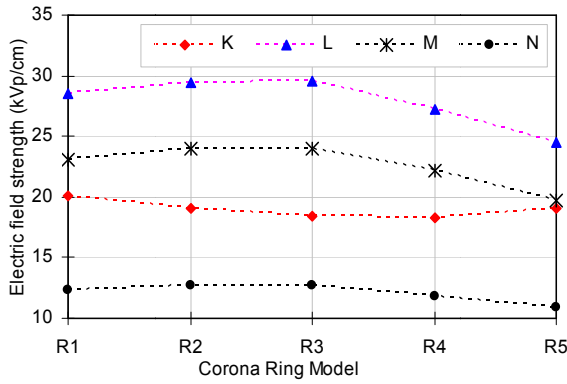


Figure 18. E_{max} on critical regions for R-type corona rings.

Similar simulations were also performed for laboratory model. Smooth aluminum tubes of 11 m length and 35 mm in diameter are positioned parallel to the laboratory earth floor to simulate the power lines (Figure 6b). Field strengths for the laboratory model are found to be less than the corresponding field strengths of service model. The E_{max} differences for C-type rings between service model and the laboratory model for regions K, L, M and N are up to 3.5, 6.0, 5.5 and 5 %, respectively. Similar field differences are also obtained for R-type rings except for the region-K, which produced 7 percent differences.

Followings summarize the overall simulation results:

- Besides the known parameters, conductor sags and ground wires effects on field distributions are also investigated for more applicable simulations.
- Maximum field strengths on the critical regions decreases for increasing corona ring tube diameter, D. Maximum field reduction (11 %) is obtained for Region-K and minimum one (5 %) is obtained for Region-N.
- Increasing installation or mounting heights increase maximum fields on Region-K but decrease them on Region-M and N. On the other hand, E_{max} on region L shows a minimum around B = 10 - 15 cm mounting height.
- Corona rings with small diameters seem to be supply better field regulation on the critical regions for B = [5-15] cm installation heights.
- Effective field control on the critical regions depends on corona ring diameter, corona tube diameter and mounting heights. While at least 5 cm of B is reasonable for 40 cm corona ring diameter, minimum 15 cm of B is required for the ring of 65 cm diameter for proper dimensioning. The smaller the corona tube diameter, the smaller the mounting height. E_{max} on the ring surface limits the minimum value of tube diameter.
- For R-type rings, corona rings with small A1 and large A3 parameters supply more field reductions on the critical regions L, M and N.
- For R-type ring, maximum field strengths on the critical regions are greater than those for C-type rings.

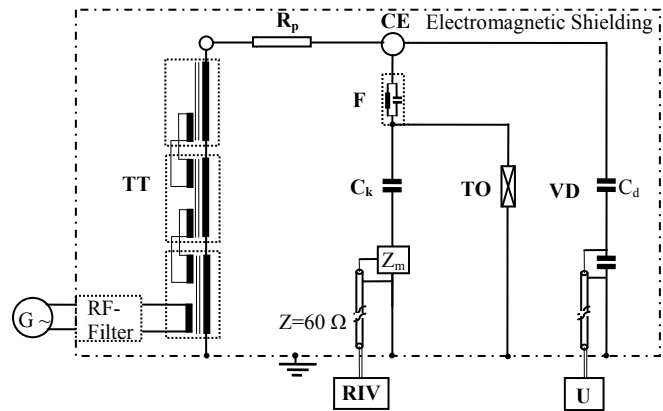
4 EXPERIMENTAL STUDIES

RIV, corona inception and ac flashover voltage tests were conducted both for experimental corona ring optimization and verification of the simulation results. Effects of both R-type and some C-type rings with respect to the impulse performance of the 380 kV V-string were also investigated previously [8, 9]. The main laboratory hall has a floor area of 25 m x 35 m and ceiling height of 22 m. 1200 kV_{rms}, 50 Hz, 1000 kVA cascaded test transformer was used for the laboratory tests. The tests were performed in an actual tower window representing the central phase as shown in Figure 19.



Figure 19. Laboratory test setup.

Equivalent test circuit of RIV and ac flashover tests is shown in Figure 20. RIV measurements were performed in accordance with IEC standard [10].



- TT : 1200 kV_{rms}, 1000 kVA, 50/150 Hz, Cascaded Test Transformer
- R_p : Protection Resistor, 9 kΩ
- CE : Central Electrode, Ø2000 mm
- F : L-C Filter (L = 250 μH, C = 100 pF)
- C_k : Coupling Capacitor, C_k = 2.5 nF
- Z_m : Measuring Impedance, Z_m = 150 Ω
- RIV : R.I.V Measuring Instrument, 0.135-30 MHz
- VD : Capacitive Voltage Divider
- U : Voltmeter
- TO : Test Object

Figure 20. RIV and ac flashover voltage test circuit.

No purely analytical methods to predict the electromagnetic noise exists since the predicting interference require some experimentally determined functions [11]. Therefore, several empirical and semi-empirical methods for evaluating RI voltages for the transmission lines have been proposed in the literature. Bundle geometry, sub-conductor diameters and maximum conductor surface gradients are generally taken into consideration for determination of the interference levels [11]. Besides transmission lines with known geometry and dimensions, interferences coming from the insulator units have also been studied for the insulators. The source and the level of the interferences caused by pin and post insulators have been presented in [12].

In order to obtain comparative results among the tested grading devices, RIV measurements were performed in a very limited time interval since the RI voltages are so sensitive to weather conditions [1, 11]. RIV tests were conducted at [13.0 - 16.3] °C temperature range and [1009-1017] mbar atmospheric pressure levels. Background noise level was 12 - 25 $\mu\text{V}/150 \Omega$ up to 350 kV_{rms} test voltages.

RIV levels versus applied voltages for C-type grading devices are shown in Figure 21. Comparisons of RIV levels at 277 kV_{rms} for six different C-type rings are shown in Figure 22. RIV levels at 277 kV_{rms} for C-type rings give the lowest values for an installation distance of B = 15 cm. The highest RIV levels are obtained for the rings installed at B = 0 cm.

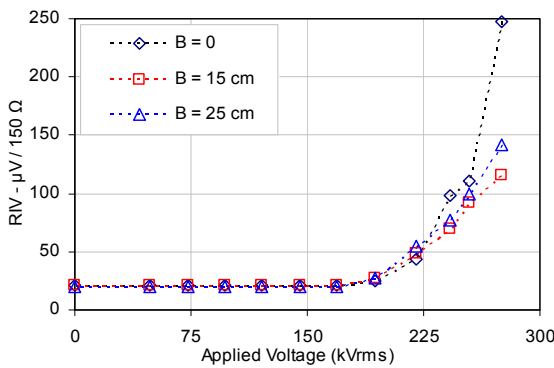


Figure 21. RIV test result for C-type corona rings (A = 55 cm, D = 5 cm).

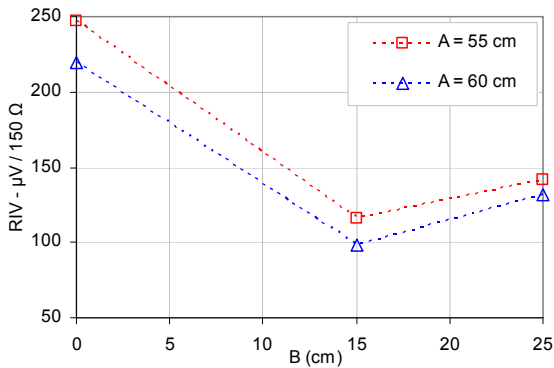


Figure 22. RIV levels at 277 kV test voltage for 2 circle type rings (D = 5 cm).

Remembering the field strength simulation results, this is mainly because of the highest field strengths on Region-L and M. The lowest RIV levels at B = 15 cm show that there is a balance between the field strengths in several different critical regions. That is, field strengths on corona ring surface gets greater than the ones on the other regions and becomes the dominant one determining the RIV level of the system. Beyond this point, RIV levels increase with an increasing installation heights. This may be explained by increasing field strengths on corona ring surfaces with increasing installation heights as given in Figures 9-10. Briefly, there is a concordance between the measured RIV levels and the maximum field strength simulations for C-type rings.

Figure 23 shows the interference level with and without corona ring case given in logarithmic scale. Corona ring usage supply significant interference reductions.

RIV levels for R-type rings are shown in Figure 24. The minimum interference levels are obtained for R5 type corona ring that also satisfies the RIV limit value. This is in concordance with the simulation results where R5 type corona ring was found to show the minimum E_{max} values at critical regions.

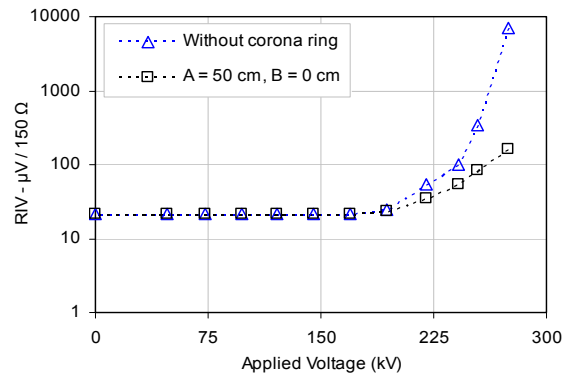


Figure 23. Effect of corona ring on RIV performance.

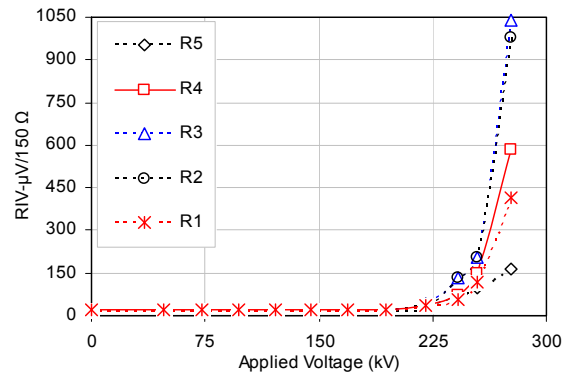


Figure 24. RIV results for R-type corona rings.

Visible corona inception voltage measurements were also performed in order to verify the validity of the simulation results. In parallel with the simulation results, visible corona discharges were first observed on Region-L and M, and

subsequently on corona ring surface for the strings where the corona rings are installed at $B = 0$ cm mounting heights. On the other hand, initial visible discharges were first observed to start on Region-K for $B = 15$ cm and $B = 25$ cm heights. Visible corona onset voltages on the ring surfaces for $A = 50$ cm/ $B = 0$ cm, $A = 50$ cm/ $B = 15$ cm and $A = 50$ cm/ $B = 25$ cm settings were measured to be 445, 425 and 385 kV_{rms} , respectively. The inception voltages for the strings without corona rings were observed to be 240, 240 and 260 kV_{rms} for Region-L, M and N, respectively.

Similar tests were also performed for R-type grading rings. Visible corona onset voltages were found to be 400, 420, 430, 420 and 415 kV_{rms} for R1, 2, 3, 4 and R5 type rings, respectively. Visible corona discharges were first initiated on Region-L and M and subsequently on the corona ring surface. These observations are also in concordance with the simulation results where the maximum field strengths were found to be on Regions-L and M.

Finally, ac flashover voltage tests for each corona ring model were also determined to see the parameter effects on the ac performance. The tests are performed at $[23.7 - 26.8]$ °C temperature range and $[1010 - 1018.5]$ mbar atmospheric pressure intervals. All the flashover voltages are corrected to normal atmospheric conditions.

Clearances for C-type ring of 50 cm diameter representative ring are shown in Figure 25. Maximum arc distance reductions for the C-type grading ring are 11 %, 11 % and 8 % along up-tower, side-tower and insulator string, respectively. It is obvious that these reductions will increase with increasing ring diameters.

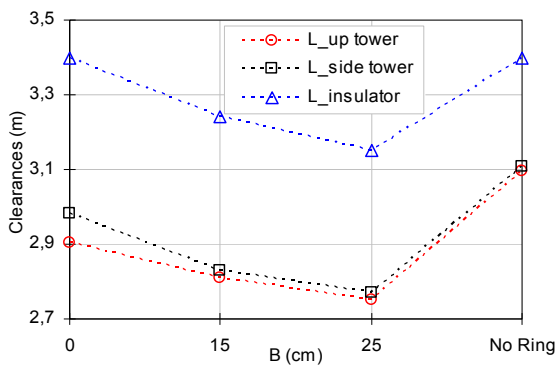


Figure 25. Variation of arc distances for C-type rings ($A = 50$ cm, $D = 5$ cm).

5 consecutive voltages causing the flashover were applied to the string. Dry ac flashover voltage level of the string without corona ring case is about 850 kV_{rms} . Flashover voltages for the C-type rings with 50, 55 and 60 cm ring diameters are shown in Figure 26. It is clear that, as corona ring diameter increases, ac flashover performance of the string decreases. Flashover voltages decrease between 8 % - 11 % for $B = 0$ case, 12 % - 14 % for $B = 15$ cm case and 14 % - 17 % for $B = 25$ cm case. Increasing both corona ring diameter and installation height decreases ac flashover voltage levels of the string.

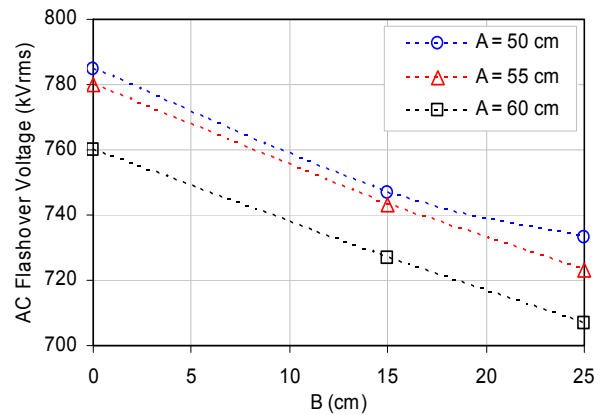


Figure 26. ac flashover voltages for C-type rings ($D = 5$ cm).

The tests showed that, the usage of corona rings reduced ac flashover voltage levels which are greater than the percentage reductions of dry arc distances. Therefore, ac flashover voltage levels of the string so the dry arc distance limit corona ring design parameters. Corona rings with smaller ring diameters installed near the live end (smaller B) provide better ac flashover voltage levels. Flashovers occurred either along up or side tower directions for $B = 0$ case. However, some flashovers were observed to occur along the insulator surface for the strings equipped with C-type corona rings installed at $B = 15$ cm and $B = 25$ cm.

Similar ac tests were also performed for R-type grading devices. Variation of clearances under different R-type rings is shown in Figure 27. R-type rings cause clearance reductions nearly 6 % along up-tower, 1.5 % alongside tower and <1 % along insulator string.

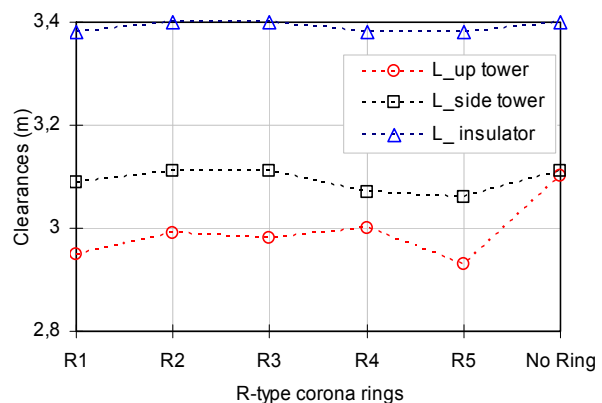


Figure 27. Variation of arc distances for R-type rings.

ac flashover voltages were measured to be 780, 765, 780, 775 and 780 kV_{rms} for R1, R2, R3, R4 and R5 type rings, respectively. Majority of the flashovers occurred along the up-tower directions. However, some side-tower flashovers were observed for R4 and R5 type rings which have larger $A3$ parameters. An example up-tower flashover for a R-type ring is illustrated in Figure 28.

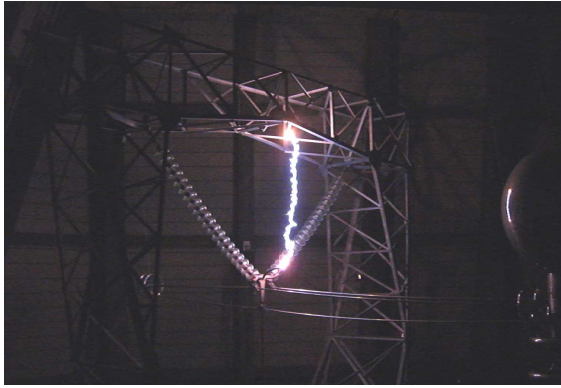


Figure 28. Up-tower flashover in a string equipped with R type ring.

R-type rings reduce the ac flashover voltages up to 10 percent which is also greater than the % clearance reductions caused by the rings.

The followings summarize the corona ring optimization with respect to corona inception voltages, RIV levels and ac flashover voltage levels:

- RIV levels are dependent on the geometry and on the location of the grading devices. Rings installed at the live end side ($B = 0$ cm) seem to be infeasible because of higher RIV levels and high electric field strengths.
- Laboratory tests showed that C-type corona rings installed at $B = 15$ cm provide the minimum RIV levels, which was previously stated by the simulations. Therefore $B = [10 - 15]$ cm range is the optimum installation height for the strings from RIV performance point of view.
- A3 is an important parameter for the R-type ring on the point of RIV performance. Corona rings with larger A3 parameter show better RIV performance.
- ac flashover performance of the string is strongly dependent on the ring settings. Decreasing arc distance causes additional decrease in ac performance. Parameter B is the dominant factor affecting the ac flashover levels.
- When RIV levels and ac flashover voltages are considered together, using corona rings with $B > 15$ cm installation heights decrease both RIV and ac performance further.
- Corona rings having 40 cm or less ring diameters are not feasible because of constructional problems. Although larger corona rings provide better RIV performances, they cause additional ac voltage reductions. Therefore, corona rings having 50 - 55 cm of ring diameters should be preferred on the point of both economic and ac performances.

5 CONCLUSIONS

This study has presented 3D-electrostatic simulations and some indoor laboratory tests for corona ring optimization used in 380 kV V-insulator string. Following conclusions were obtained from the overall study:

1. Besides the known parameters such as line lengths and adjacent phases, conductor sags are also found to be effective parameter on the field distributions.

2. Effective control of the maximum fields on the critical regions depends on corona tube diameter, corona ring diameter and installation heights.
3. Increasing corona tube diameter, D , decreases the maximum fields on the critical regions to some extent. However, E_{\max} on the ring surface are the most sensitive to the tube diameter. As the tube diameter decreases, smaller mounting heights are required for effective field control. $D < 4$ cm is not reasonable because of excessive maximum field occurrence on the ring surface and $D > 5$ cm is not also suitable both for effective field control and economic points of view.
4. Corona ring installation height, B , is found to be the most effective parameter dominating the optimization. The value of B is dependent on the corona ring diameter. The larger the corona ring diameters, the larger the installation heights for the proper field regulation. At least $[5 - 15]$ cm of parameter B is required for $[40 - 65]$ cm of parameter A for proper dimensioning. On the other hand, E_{\max} on region L shows a minimum around $B = 10 - 15$ cm mounting height.
5. R-type rings with small A1 and large A3 parameters supply more field reductions on the critical regions. Bigger than 70 cm A3 parameter is required for effective field control for R-type rings.
6. RIV and visible corona inception test results are found to be in good concordance with simulated maximum field strengths. They have verified the fact that C-type corona rings installed at $B = 10 - 15$ cm provide the minimum RIV levels, which was previously stated by the simulations.
7. A good coverage of the critical regions so R-type rings with larger R3 parameters show better RIV performances.
8. Decreasing arc distance causes additional decrease in ac flashover performance. Parameter B is the dominant factor affecting the ac flashover levels.
9. Increasing RIV levels and decreasing ac flashover performances under larger B parameter limit the value of B. $B > 15$ cm is not supply any improvement both for field regulation and RIV levels. Moreover, using the rings with larger B parameter can cause insulator surface flashovers.
10. Corona rings having 40 cm or less ring diameters are not feasible because of constructional problems for cap-and-pin type insulators. Although larger corona rings provide better RIV performances, they cause additional ac voltage reductions. Therefore, 50 - 55 cm of ring diameters should be preferred on the point of both economic and ac flashover performances.

APPENDIX

SOFTWARE USED

Boundary element based commercial software, Coulomb, [13] is used to calculate the field distributions. Before the simulations, different number of 2D elements for surfaces and 1D elements for segments are tested for reasonable accuracy

and computational time. Total 50.000-2D triangular elements and 6000-1D line elements are found to provide reasonable accuracy in an average computation time of 4 hours by a Pentium-4, 2.4 GHz PC of 64 Bit Processing System with 8 GB of RAM.

ACKNOWLEDGMENT

The authors would like to thank the Turkish National Electric Power Transmission Company for their support and encouragement for the study. They would also like to thank to Fuat Kulunk High Voltage Laboratory staff for their patient supports during the tests.

REFERENCES

- [1] P. S. Maruvada, *Corona Performance of High Voltage Transmission Lines*, Research Studies Press, Baldock, England, p. 111, p. 144, 2000.
- [2] W. Sima, F. P. Espino-Cortes, A. C. Edward and H. S. Jayaram, "Optimization of Corona Ring Design for Long-Rod Insulators Using FEM Based Computational Analysis", IEEE Intern. Sympos. Electr. Insul., pp. 480–483, 2004.
- [3] W. Sima, K. Wu, Q. Yang and C. Sun, "Corona Ring Design of ± 800 kV DC Composite Insulator Based on Computer Analysis", IEEE Intern. Conf. Electr. Insul. Dielectr. Phenomena, pp. 457–460, 2006.
- [4] E. Brasca, E. Comellini and D. Dellolio, "Power Arc on Insulator Strings: Testing Procedures and Design of Guard Devices for HV Transmission Lines", IEEE Trans. Power App. Syst., Vol. 89, pp. 420–428, 1970.
- [5] T. Zhao and M. G. Comber, "Calculation of Electric Field and Potential Distribution Along Nonceramic Insulators Considering the Effects of Conductors and Transmission Towers", IEEE Tran. Power Delivery, Vol. 15, pp 313–318, 2000.
- [6] J. Bradbury, G. F. Kuska, D. J. Tarr, "Sag and Tension Calculations for Mountainous Terrain", IEE Proc. Generation, Transmission and Distribution" Vol. 129, pp. 213-220, 1982.
- [7] R. C. Landy and J. P. Reynders, "Corona Inception on Cap-and-Pin Insulators in Clean Environments", 13th Intern. Sympos. High Voltage Eng., Netherlands, pp. 1-6, 2003.

- [8] S. Ilhan and A. Ozdemir, "Flashover Performance of 380 kV V-Strings with Composite Insulators under Lightning and Switching Impulses", IEEE Bucharest PowerTech, Romania, pp. 1-6, 2009.
- [9] S. Ilhan and A. Ozdemir, "Flashover Performance of 380 kV V-Strings with Cap-and-Pin Type Insulators under Lightning and Switching Impulses", 16th Intern. Sympos. High Voltage Eng., South Africa, Paper C-38, pp. 727-732, 2009.
- [10] IEC Overhead Lines - Requirements and tests for fittings, IEC Standard 61284, 1997-09-17.
- [11] R. G. Olsen, S. D. Schennum and V. L. Chartier, "Comparison of Several Methods for Calculation Power Line Electromagnetic Interference Levels and Calibration with Long-term Data", IEEE Trans. Power Delivery, Vol. 7, pp. 903-913, 1992.
- [12] E. Kuffel, R. N. Allan and I. Aktekin, "Radio Interference from High Voltage Insulators and Factors which Affect the Interference Levels", Proc. IEE. Vol. 112, pp. 925-930, 1965.
- [13] *Integrated Engineering Software—Coulomb 3D, Users and Technical Manual for, Version 7.0*, Winnipeg: Enginia Research Inc., 2008.



Suat Ilhan (M'10) was born in Malatya, Turkey in 1979. He received the B.Sc. and M.Sc. degrees in electrical engineering from Istanbul Technical University, Istanbul, Turkey in 2001 and 2004, respectively. He is currently a research assistant at the same university. His main research interests are numerical analysis of electrical fields, insulation design of electric power systems, measurement of partial discharge and electromagnetic interferences.



Aydogan Ozdemir (M'98) was born in Artvin, Turkey in January 1957. He received the B.Sc., M.Sc. and Ph.D. degrees in electrical engineering from Istanbul Technical University, Istanbul, Turkey in 1980, 1982 and 1990, respectively. He is currently a full professor at the same university. His current research interests are in the area of electric power system with emphasis on reliability analysis, modern tools.